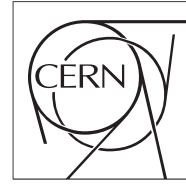


The Compact Muon Solenoid Experiment
Conference Report

Mailing address: CMS CERN, CH-1211 GENEVA 23, Switzerland



16 July 2013 (v4, 22 August 2013)

Jet Quenching with ATLAS and CMS

Pelin Kurt Garberson for the ATLAS and CMS collaborations

Abstract

An overview of the most recent results on jet quenching physics obtained using PbPb collision data collected with the ATLAS and the CMS experiments at $\sqrt{s_{NN}} = 2.76$ TeV will be presented. These measurements make use of many different observables, including momentum imbalance of dijet and photon-jet events, nuclear modification factors R_{AA} and R_{CP} , as well as jet fragmentation functions, jet shapes, and flavor dependence of jet quenching. The measurements in PbPb collisions will be compared to those obtained from pp collisions at the same center-of-mass energy. The effects of the parton energy loss in the hot and dense medium probed with the different observables will be discussed.

Presented at *INPC2013 25th International Nuclear Physics Conference*

Jet Quenching with ATLAS and CMS

Pelin Kurt¹ for the CMS Collaboration e-mail: pkurt@cern.ch

¹University of Illinois at Chicago, USA

Abstract. An overview of the most recent results on jet quenching physics obtained using PbPb collision data collected with the ATLAS and the CMS experiments at $\sqrt{s_{NN}}=2.76$ TeV will be presented. These measurements make use of many different observables, including momentum imbalance of dijet and photon-jet events, nuclear modification factors R_{AA} and R_{CP} , as well as jet fragmentation functions, jet shapes, and the flavor dependence of jet quenching. The measurements in PbPb collisions will be compared to those obtained from pp collisions at the same center-of-mass energy. The effects of the parton energy loss in the hot and dense medium probed with the different observables will be discussed.

1 Introduction

Heavy ion collisions at the Large Hadron Collider (LHC) allow one to study the phases of nuclear matter predicted by the theory of the strong interaction Quantum Chromodynamics (QCD) [1, 2]. Jets associated with the hard scattering of partons are a powerful probe of the hot, dense matter created in heavy-ion collisions. This medium is commonly referred to as a Quark-Gluon Plasma (QGP). The partons lose energy while traversing the medium via elastic processes (collisional parton energy loss) or inelastic processes (radiative parton energy loss) [3]. At RHIC, indirect measurements of energy loss in the medium (“jet quenching”) have been made by studying high momentum jet fragmentation products [4, 5]. More recently, the ATLAS [6] and the Compact Muon Solenoid (CMS) [7] detectors have been used to study for parton energy loss in the quark-gluon plasma with leading particle and jet coincidence measurements. The ATLAS and the CMS detectors are general purpose particle experiments operating at the LHC. These detectors are built to be sensitive to a wide-variety of physics processes, and are well suited for the study of heavy-ion collisions. We present some selected measurements related to parton energy loss in PbPb collisions at a nucleon-nucleon center-of-mass energy of $\sqrt{s_{NN}}=2.76$ TeV collected in 2010 and 2011 using the ATLAS and CMS detectors.

2 Experimental Techniques

The heavy-ion analyses at ATLAS and CMS share some common experimental methods. In these measurements it is common to first perform a measurement where the medium is present, and then to make the same measurement in pp or pp-like collisions, and finally compare to study the medium-induced modifications. For this comparison, a pp reference data (at the same center-of-mass energy) was collected at the LHC.

The capabilities of the ATLAS and CMS detector allow us to investigate various hard probes, using excellent tracking, calorimetric, and muon systems which cover a large range in pseudorapidity. All of these detectors have sufficient granularity and resolution to function well even in the highest multiplicities encountered in PbPb collisions.

It is also important to note that heavy ions are extended objects, so the impact parameter is an important characterization of the events. The centrality of the collisions is defined as a fraction of the total nucleus-nucleus inelastic cross section, with 0% denoting the most central collisions with impact parameter 0, and 100% - the most peripheral collisions. In these analyses, centrality was determined from minimum bias events based on the total energy from both forward hadronic calorimeters [8, 9]. The more frequent peripheral events with a large impact parameter produce very few particles, while the central ones with a small impact parameter produce many more particles because of the increased number of nucleon-nucleon interactions.

3 Results

In contrast to pp collisions, a large fraction of imbalanced dijet transverse momentum has been observed in PbPb collisions at $\sqrt{s_{NN}} = 2.76$ TeV. This observation was first reported by ATLAS [8] using a data sample corresponding to an integrated luminosity of $1.7 \mu b^{-1}$, where the dijet momentum balance has been quantified in different centrality bins using an asymmetry ratio $A_j = \frac{E_{T_1} - E_{T_2}}{E_{T_1} + E_{T_2}}$, where E_{T_1} is the transverse energy of the leading jet and required to be $E_{T_1} > 100$ GeV, and E_{T_2} is the transverse energy of the subleading jet in the opposite hemisphere with $E_{T_2} > 25$ GeV. In Fig. 1 the top panel shows that the dijet asymmetry in peripheral PbPb events is similar to that in both pp and simulated events. However, as the events become more central, the PbPb data distributions develop different characteristics, indicating an increased rate of highly asymmetric dijet events. In the bottom panel, the azimuthal-angle between the dijet events are shown for different centrality classes. It is clear that the leading and subleading jets are primarily back-to-back in all centrality bins. However, a systematic increase is observed in the rate of second jets at large angles relative to the recoil direction as the events become more central. This is due to the jet-quenching effect which can cause some jets to become lower in p_T than jets from a second hard scattering. This can result in an association of a leading jet to a jet from a different hard scattering instead of the proper rebound jet. As expected, this effect is quite visible in data where the medium effect is present.

In a more detailed study of the parton energy loss mechanism [9], CMS has investigated the redistribution of the quenched jet energy using the transverse momentum balance of charged tracks projected onto the direction of the leading jet axis, defined as $p_T^{\parallel} = \sum_i -p_T^i \cos(\phi_i - \phi_{\text{Leading Jet}})$, where the sum is evaluated over all tracks with $p_T > 0.5$ GeV/c and $|\eta| < 2.4$. The results were then averaged over the event ensemble to obtain $\langle p_T^{\parallel} \rangle$. No explicit background subtraction is applied in this method, as the heavy-ion underlying event is not expected to give a net p_T contribution along the leading jet axis. Fig. 2 (left) shows $\langle p_T^{\parallel} \rangle$ as a function of A_j for the most central PbPb collisions (0–30%). Even for events with a very unbalanced dijet (large A_j values), the total summed projected momentum of all the included tracks (solid circles) is close to zero. The colored bands (with vertical bars for statistical uncertainties) show the summed momentum for tracks restricted to specific p_T ranges. The sum for tracks with $p_T > 8$ GeV/c is strongly negative, indicating that they carry excess momentum in the direction of the leading jet. This negative excess is balanced by the almost equally strong positive contribution of tracks in the 0.5 GeV/c regions. Tracks in the intermediate range, $2 < p_T < 8$ GeV/c, also tend to carry excess momentum in the direction of the subleading jet, but to a lesser degree. The main conclusion here is that a large fraction of the momentum balance of the jets in unbalanced events is carried by low- p_T particles at large radial distance to the jet axis [9].

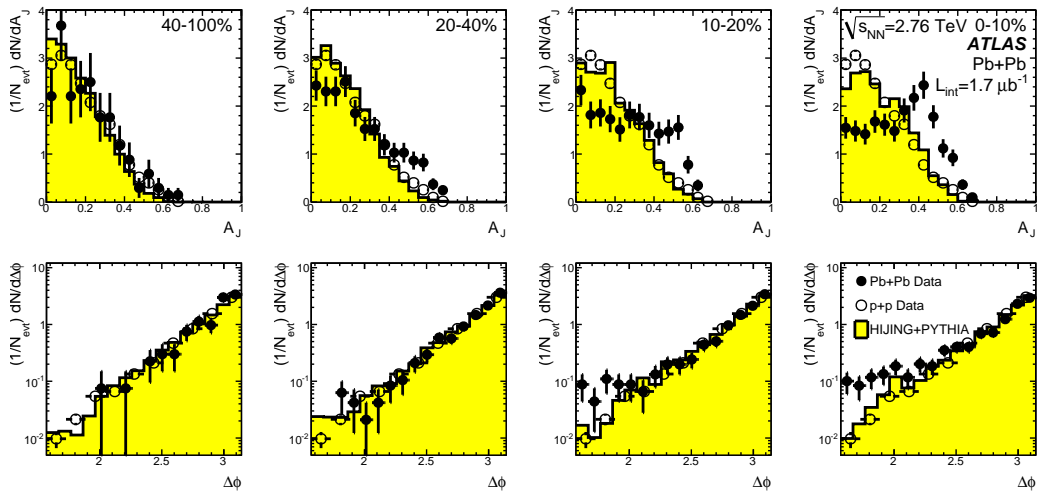


Figure 1. (top) Dijet asymmetry distributions for data (points) and unquenched heavy ion simulation with superimposed PYTHIA pp dijets (solid yellow histograms), as a function of collision centrality (left to right from peripheral to central events). Proton-proton data from $\sqrt{s_{NN}} = 7$ TeV, analyzed with the same jet selection, is shown as open circles. (bottom) Distribution of $\Delta\phi$, the azimuthal angle between the two jets, for data and heavy ion simulation, also as a function of centrality.

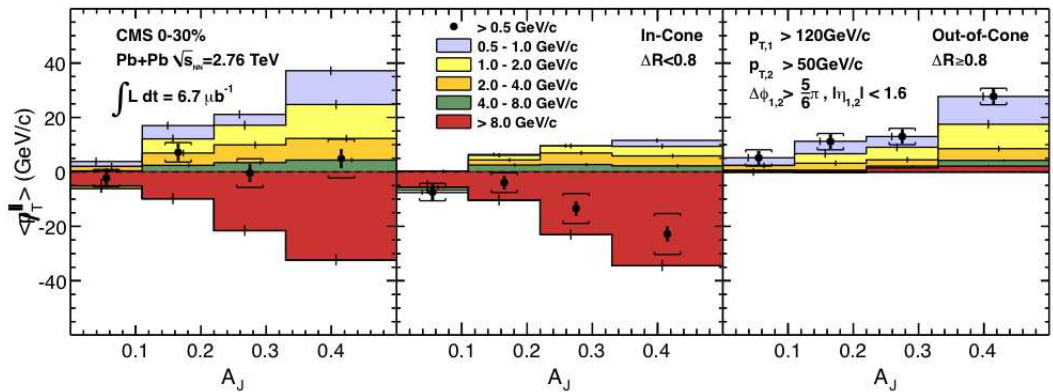


Figure 2. (Left) Average missing transverse momentum, $\langle p_T^{\parallel} \rangle$, for tracks with $p_T > 0.5$ GeV/c, projected onto the leading jet axis (solid circles). The $\langle p_T^{\parallel} \rangle$ values are shown as a function of dijet asymmetry for the 30% most central events. (Middle) The $\langle p_T^{\parallel} \rangle$ values as a function of A_J inside ($\Delta R < 0.8$) one of the leading or subleading jet cones. (Right) $\langle p_T^{\parallel} \rangle$ outside ($\Delta R > 0.8$) the leading and subleading jet cones. For the solid circles, vertical bars and brackets represent the statistical and systematic uncertainties, respectively. Colored bands, with vertical bars for statistical uncertainties, show the contribution to $\langle p_T^{\parallel} \rangle$ for five ranges of track p_T .

While studies using dijets benefit from the large dijet production cross section, the energy loss of both partons makes the determination of the amount of energy lost by each parton more difficult. Correlations between isolated photons and jets have been proposed in the literature as the “golden channel” to study jet energy loss. This is because the photon retains the kinematic information of the hard scattering since it is not expected to interact with the medium. In addition, the energy resolution for photons is better, making the photon an ideal object against which to compare the jet. In order to quantify any angular broadening, the PbPb data were compared to both pp data and a PYTHIA+HYDJET reference which included the effect of the underlying PbPb event but no parton energy loss. Similar to dijet events, no angular broadening was observed beyond that seen in the pp data and MC reference at all centralities. Further details about the first measurement of isolated-photon+jet correlations in $\sqrt{s_{NN}} = 2.76$ TeV pp and PbPb collisions with CMS can be found elsewhere [10].

Energy loss of the parent partons in the medium may reduce or “suppress” the production of jets at a given transverse momentum. Such energy loss is expected to increase with medium temperature and with increasing path length of the parton in the medium [11]. As a result, there should be more suppression in “central” Pb+Pb collisions, which have nearly complete overlap between the incident nuclei, and little or no suppression in “peripheral” collisions where the nuclei barely overlap. The jet suppression may be quantified using the central-to-peripheral ratio, R_{CP} , the ratio of the per-event jet yields divided by the number of nucleon-nucleon collisions in a given centrality bin to the same quantity in a peripheral centrality bin formulated as $R_{CP} = \frac{\frac{1}{N_{coll}} \frac{1}{N_{ev}} \frac{dN}{dp_T} |_{cent}}{\frac{1}{N_{coll}} \frac{1}{N_{ev}} \frac{dN}{dp_T} |_{60-80\%}}$. The N_{coll} is the average number of nucleon-nucleon collisions occurring in heavy-ion (AA) collisions, calculated with a Glauber model with a detailed description of the nuclear collision geometry. This measurement was performed by both ATLAS and the CMS experiments. An unfolding procedure is also applied to account for the effects of detector resolution. The reconstructed E_T spectrum in each centrality bin is unfolded to the particle level, taking into account the migration between bins that arises due to experimental jet energy resolution. Results are shown for the ATLAS experiment [12] in Fig. 3. This figure shows the unfolded R_{CP} values obtained for $R=0.2$ and $R=0.4$ jets (reconstructed with the anti- k_T algorithm) as a function of the jet p_T in four bins of collision centrality. The R_{CP} values for all centralities and for both jet radii are observed to have at most a weak variation with p_T . For the 0-10% centrality bin the R_{CP} values for both jet radii show a factor of about two suppression in the $1/N_{coll}$ -scaled jet yield. For more peripheral collisions, R_{CP} increases at all jet p_T relative to central collisions, with the R_{CP} values reaching 0.9 for the 50-60% centrality bin.

Another interesting analysis is a measurement of the jet flavor dependence of the jet quenching, which is expected to depend on the flavor of the initial parton. Gluon jets are expected to be quenched more strongly than light quark jets due to the larger color factor for gluon emission from gluons than from quarks. On the other hand, jets initiated by heavy quarks, particularly bottom quarks, are expected to radiate less than light ones. To measure this flavour dependence, the CMS collaboration has applied a b-jet identification algorithm for the first time in heavy ion collisions to perform such a measurement [13]. The purity of b-jet tagging is determined from template fits to the secondary vertex invariant mass distribution, and the efficiency of the secondary vertex tagging is estimated in a data-driven technique. The fraction of b-jet among inclusive jets is measured as a function of transverse momentum after purity and efficiency corrections. The fraction of b-jets in pp and PbPb collisions are comparable, with no p_T dependence, indicating that b-quark jets are quenched similar to the light quark jets, i.e. the R_{AA} value is ≈ 0.5 . These measurements have significant statistical uncertainties at present. The addition of more statistics, along with a more precise calibration of tagging efficiencies and fit template shapes, may lead to significant improvements in precision in the future.

A differential measurement has been performed to test the effects of the medium using a jet shape observable at the CMS experiment. The jet shapes are a sensitive tool for the characterization of the

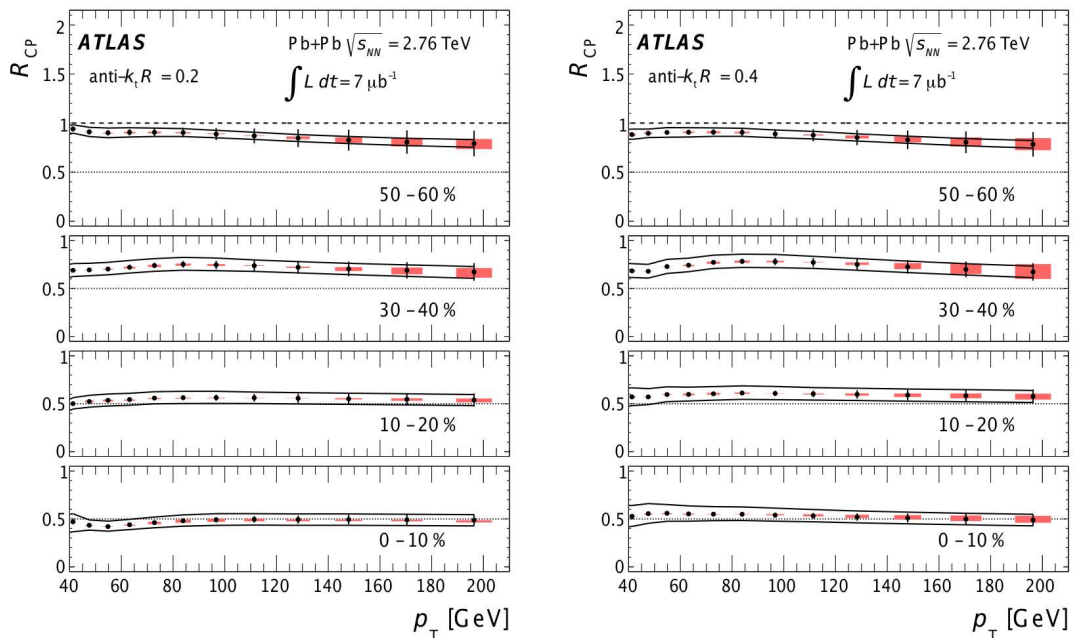


Figure 3. Unfolded R_{CP} values as a function of jet p_T for $R = 0.2$ (left) and $R = 0.4$ (right) anti- k_T jets in four bins of collision centrality. The error bars indicate statistical errors from the unfolding, and the shaded boxes indicate unfolding regularization systematic errors that are partially correlated between points. The solid lines indicate systematic errors that are fully correlated between all points. The horizontal width of the systematic error band is chosen for presentation purposes only. Dotted lines indicate $R_{CP} = 0.5$, and the dashed lines on the top panels indicate $R_{CP} = 1$.

parton-medium interactions by utilizing the energy flow inside the jet. Predictions have been made that the jet shapes will become wider due to quenching effects [14]. We present the first experimental test of this prediction. For this measurement, jets are reconstructed using the anti- k_T jet clustering algorithm [15], with a resolution parameter $R=0.3$ for both PbPb and pp collisions at 2.76 TeV. Individually calibrated particle candidates are used as inputs to the jet clustering algorithm. These particle candidates are reconstructed using the CMS particle flow (PF) algorithm [16]. The jet shape is defined as the average fraction of the jet transverse momentum within a cone of a given size r around the jet axis. The jet shapes can be studied by using an integrated or a differential distribution. The shapes are defined as the average fraction of the transverse momentum contained inside an annulus of an inner radius $r_a = r - \delta r/2$ and an outer radius $r_b = r + \delta r/2$ as specified in the following equation

$$\rho(r) = \frac{1}{\delta r} \frac{\sum_{r_a < r_i < r_b} p_{T,i}}{\sum_{r_i < R} p_{T,i}}, \quad (1)$$

where δr is used as the annulus size, which is 0.05. The sums run over the reconstructed particles, with the distance $r_i = \sqrt{(\eta_i - \eta_{jet})^2 + (\phi_i - \phi_{jet})^2}$ relative to the jet axis described by η_{jet} , ϕ_{jet} , and R .

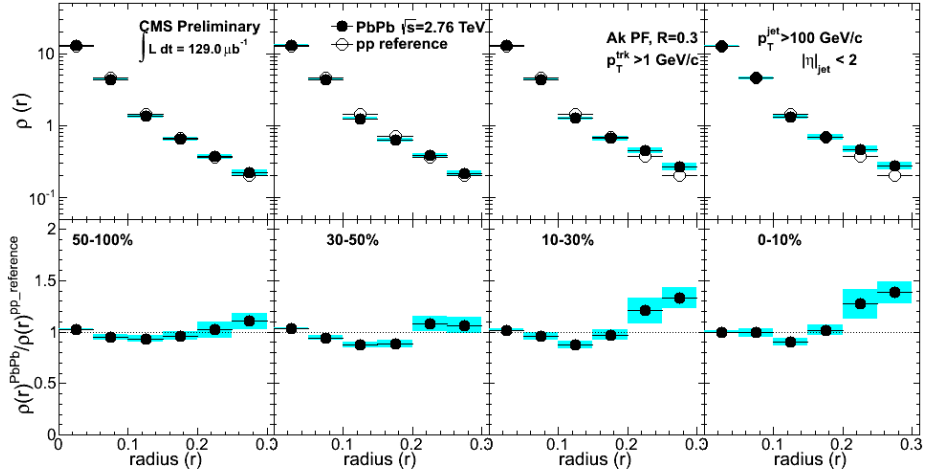


Figure 4. Differential jet shapes in PbPb and pp collisions are presented for different centrality bins for $p_T^{jet} > 100$ GeV with track $p_T > 1$ GeV are shown in the top panels. Results from data are shown as black points while the open circles show the reference pp. In the bottom row, the ratio of the PbPb and pp jet shapes is shown. The blue band shows the total systematic uncertainty while the error bars indicate the statistical errors.

A small cone size ($R=0.3$) was used for the jet reconstruction in order to suppress the underlying-event contribution in the high multiplicity PbPb environment. All charged particles that pass a $p_T > 1$ GeV/c threshold are used to reconstruct jet shapes. Corrections for the tracking inefficiency are applied. The hot-and-dense medium is expected to modify a measured jet shape in two ways. First, the partons that fragment into jets interact with the medium directly. Secondly, the soft particle production from the underlying event adds many extra particles to the jet, predominantly at low momentum. This latter effect produces a background that must be subtracted. In order to subtract the heavy-ion background, an η -reflection technique [17] was used. In order to understand the medium-parton interactions we compare the PbPb jet shapes results with those obtained from a pp reference. For a direct comparison between pp and PbPb collisions, the jet momentum resolution deterioration in PbPb events is taken into account. For this purpose, the reconstructed p_T of every jet in the pp data is smeared by the quadratic difference of the jet energy resolution obtained in PbPb and pp. The resulting jet p_T spectrum is compared to the spectra in PbPb collisions of different centrality to determine a p_T -dependent weight, which is applied on a jet-by-jet basis to obtain reference jet-shape distributions. This process is needed to ensure that the comparison is free of detector effects and that the kinematic range of the jets included in the comparison is the same.

The measured differential jet shapes for PbPb and pp reference data are presented in Fig. 4 for different centrality bins, ranging from most-peripheral (50–100%) to most central (0–10%). The bottom panel shows the ratio of the PbPb jet shapes to the jet shapes for a pp reference obtained for the respective selections. Deviations from unity indicate modification of jet structure in the nuclear medium. We note that the jet shape spectra are normalized to unity. As a result, an excess at one distance r from the jet axis has to be compensated by a depletion in another region. In all centrality classes, the ratios have a concave shape, which is more pronounced in the more central collisions. In central collisions (10–30% and 0–10%), an excess at large radius $r > 0.2$ emerges, indicating a moderate broadening of the jets in the medium. This result is consistent with previous studies in CMS which find that the energy that the jets lose in the medium is redistributed at large distances from the jet axis outside the jet cone [9].

In another differential CMS measurement the fragmentation functions, defined as the distribution of the fraction of the jet momentum carried by tracks of different p_T , are determined [17]. The

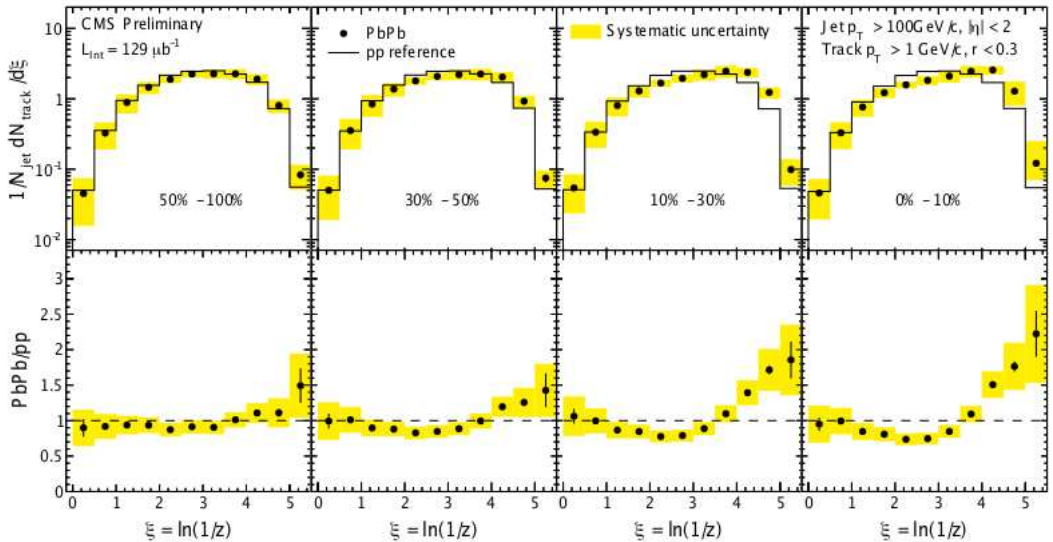


Figure 5. The top row shows the jet fragmentation functions in PbPb in bins of increasing centrality, overlaid with pp. Jets are required to have p_T above 100 GeV/c, and tracks to have p_T above 1 GeV/c. The PbPb data is shown in the top row in four increasing centrality bins from left to right. The bottom row shows the ratio of each PbPb fragmentation function to its pp reference.

fragmentation function is formulated with ξ , defined as $\xi = \ln \frac{1}{z}$; $z = \frac{p_{\parallel}^{track}}{p_T^{jet}}$ where p_{\parallel}^{track} is the momentum component of the track along the jet axis, and p_T^{jet} is the transverse momentum of the reconstructed jet, respectively. The event selection and analysis procedure are the same as in inclusive jet shapes analysis. In order to quantify the medium-related effects, the results are compared to the references based on pp data. The upper panel of Fig. 5 shows the reconstructed fragmentation functions in pp and PbPb data. The bottom panel shows that the modification of the fragmentation function of jets grows with the collision centrality. In the 50-100% bin, the ratio of PbPb/pp is flat at unity which means no modification. However, an excess in high ξ is observed for more central events. This implies that for central collisions the spectrum of particles in a jet has an enhanced contribution of soft particles compared to one from pp collisions.

4 Conclusion

The ATLAS and CMS collaborations have performed many interesting measurements in PbPb collisions. All these measurements in PbPb collisions are presented and compared with observations in 2.76 TeV pp collisions to probe for distortions from energy loss in the hot and dense medium. In summary, the fraction of dijets in which the momentum of the leading and subleading jets are significantly unbalanced rises dramatically for more central PbPb collisions, consistent with significant quenching of hard partons. A large fraction of the momentum “missing” from the lower energy jet is carried by low- p_T particles at relatively large angles with respect to the jet axis. The photon-jet correlation studies support the dijet quenching picture further. Measurement of b-jets shows that the

heavy quark jets are quenched similar to light quark jets, with no strong dependence on jet p_T . A clear centrality dependent modification of the inclusive jet rates, shapes and fragmentation function in PbPb collisions is now revealed. Since many of these observables have low correlation to one-another they serve as useful independent confirmations of the quenching properties, and indicate a consistent view of the hot and dense medium.

References

- [1] D. A. Appel, “Jets as a probe of quark-gluon plasmas”, Phys. Rev. D33 (1986) 717. doi:10.1103/PhysRevD.33.717.
- [2] J. P. Blaizot and L. D. McLerran, “Jets in Expanding Quark - Gluon Plasmas”, Phys. Rev. D34 (1986) 2739. doi:10.1103/PhysRevD.34.2739.
- [3] J. D. Bjorken, “Energy loss of energetic partons in QGP: possible extinction of high p_T jets in hadron-hadron collisions”, (1982). FERMILAB-PUB-82-059-THY.
- [4] PHENIX Collaboration, “Suppression of Hadrons with Large Transverse Momentum in Central Au+Au Collisions at 130GeV”, Phys. Rev. Lett. 88, 022301 (2001).
- [5] STAR Collaboration, “Direct observation of dijets in central Au+Au collisions at 200 GeV”, Phys.Rev.Lett. 97 (2006) 162301.
- [6] ATLAS Collaboration, “The ATLAS experiment at the CERN LHC”, JINST 3 (2008) S08003. doi:10.1088/1748-0221/3/08/S08003.
- [7] CMS Collaboration, “The CMS experiment at the CERN LHC”, JINST 3 (2008) S08004. doi:10.1088/1748-0221/3/08/S08004.
- [8] ATLAS Collaboration, “Observation of a Centrality-Dependent Dijet Asymmetry in Lead-Lead Collisions at $\sqrt{s_{NN}} = 2.76$ TeV with the ATLAS Detector at the LHC Phys. Rev. Lett. 105 (2010) 252303.
- [9] CMS Collaboration, “Observation and studies of jet quenching in PbPb collisions at 2.76 TeV”, Phys. Rev. C 84 (2011) 024906.
- [10] CMS Collaboration, “Studies of jet quenching using isolated-photon+jet correlations in PbPb and pp collisions at $\sqrt{s_{NN}} = 2.76$ TeV Phys. Lett. B 18 (2013) 773.
- [11] N. Armesto, B. Cole, C. Gale, W.A. Horowitz, P. Jacobs, et al., Phys. Rev. C 86 (2012) 064904.
- [12] ATLAS Collaboration, “Measurement of the jet radius and transverse momentum dependence of inclusive jet suppression in lead-lead collisions at $\sqrt{s_{NN}} = 2.76$ TeV with the ATLAS detector”, Phys. Lett. B 719 (2013) 220-241.
- [13] CMS Collaboration, “Measurement of the b-jet to inclusive jet ratio in PbPb and pp collisions at $\sqrt{s_{NN}} = 2.76$ TeV with the CMS detector”, CMS Physics Analysis Summary CMS-PAS-HIN-12-003 (2012).
- [14] Vitev, I. et. al., “A theory of jet shapes and cross sections: from hadrons to nuclei”, JHEP 0811:093, 2008.
- [15] M. Cacciari, G. Salam, and G. Soyez, “The anti- k_T jet clustering algorithm”, JHEP 04 (2008) 063.
- [16] CMS Collaboration, “Particle-Flow Event Reconstruction in CMS and Performance for Jets, Taus, and E_T^{miss} ”, CMS Physics Analysis Summary CMS-PAS-PFT-09-001 (2009).
- [17] CMS Collaboration, “Detailed Characterization of Jets in Heavy Ion Collisions Using Jet Shapes and JetFragmentation Functions”, (2012) CMS-PAS-HIN-12-013.